Radiology

ORIGINAL RESEARCH • MEDICAL PHYSICS

Multicenter Quantification of Radiation Exposure and Associated Risks for Prostatic Artery Embolization in 1476 Patients

Raj Ayyagari, MD • Saumik Z. Rahman, MD • Kevin Grizzard, PhD • Adel Mustafa, PhD • Lawrence H. Staib, PhD • Rasha S. Makkia, PhD • Shivank Bhatia, MD • Tiago Bilhim, MD, PhD • Francisco C. Carnevale, MD, PhD • Clifford Davis, MD • Aaron Fischman, MD • Ari Isaacson, MD • Timothy McClure, MD • Justin McWilliams, MD • Charles Nutting, DO • Andrew Richardson, MD, MBA • Riad Salem, MD, MBA • Marc Sapoval, MD, PhD • Hyeon Yu, MD

From the Boston Medical Center, 75 Albany Street, Boston, MA 02118 (R.A.); Yale University School of Medicine, New Haven, Conn (S.Z.R., K.G., A.M., L.H.S., R.S.M.); University of Miami Miller School of Medicine, Miami, Fla (S.B., A.R.); Centro Hospitalar Universitário de Lisboa Central, Lisbon, Portugal (T.B.); Universidade de São Paulo Faculdade de Medicina, São Paulo, Brazil (F.C.C.); University of South Florida Morsani College of Medicine, Tampa, Fla (C.D.); Icahn School of Medicine at Mount Sinai, New York, NY (A.F.); Prostate Centers Raleigh, Raleigh, NC (A.I.); Weill Cornell Medical College, New York, NY (T.M.); University of California Los Angeles David Geffen School of Medicine, Los Angeles, Calif (J.M.); Endovascular Consultants of Colorado, Lone Tree, Colo (C.N.); Northwestern University Feinberg School of Medicine, Evanston, Ill (R.S.); Assistance Publique-Hôpitaux de Paris, Hôpital Européen Georges-Pompidou, Paris, France (M.S.); and The University of North Carolina at Chapel Hill School of Medicine, Chapel Hill, NC (H.Y.). Received July 24, 2023; revision requested September 18; revision received January 11, 2024; accepted January 19. **Address correspondence to** R.A. (email: *Raj.Ayyagari@BMC.org*).

Conflicts of interest are listed at the end of this article.

See also the editorial by Mahesh in this issue.

Radiology 2024; 310(3):e231877 • https://doi.org/10.1148/radiol.231877 • Content codes: NM CT

Background: Prostatic artery embolization (PAE) is a safe, minimally invasive angiographic procedure that effectively treats benign prostatic hyperplasia; however, PAE-related patient radiation exposure and associated risks are not completely understood.

Purpose: To quantify radiation dose and assess radiation-related adverse events in patients who underwent PAE at multiple centers.

Materials and Methods: This retrospective study included patients undergoing PAE for any indication performed by experienced operators at 10 high-volume international centers from January 2014 to May 2021. Patient characteristics, procedural and radiation dose data, and radiation-related adverse events were collected. Procedural radiation effective doses were calculated by multiplying kerma-area product values by an established conversion factor for abdominopelvic fluoroscopy-guided procedures. Relationships between cumulative air kerma (CAK) or effective dose and patient body mass index (BMI), fluoroscopy time, or radiation field area were assessed with linear regression. Differences in radiation dose stemming from radiopaque prostheses or fluoroscopy unit type were assessed using two-sample *t* tests and Wilcoxon rank sum tests.

Results: A total of 1476 patients (mean age, 69.9 years ± 9.0 [SD]) were included, of whom 1345 (91.1%) and 131 (8.9%) underwent the procedure with fixed interventional or mobile fluoroscopy units, respectively. Median procedure effective dose was 17.8 mSv for fixed interventional units and 12.3 mSv for mobile units. CAK and effective dose both correlated positively with BMI (R^2 = 0.15 and 0.17; P < .001) and fluoroscopy time (R^2 = 0.16 and 0.08; P < .001). No radiation-related 90-day adverse events were reported. Patients with radiopaque implants versus those without implants had higher median CAK (1452 mGy [range, 900–2685 mGy] vs 1177 mGy [range, 700–1959 mGy], respectively; P = .01). Median effective dose was lower for mobile than for fixed interventional systems (12.3 mSv [range, 8.5–22.0 mSv] vs 20.4 mSv [range, 13.8–30.6 mSv], respectively; P < .001).

Conclusion: Patients who underwent PAE performed with fixed interventional or mobile fluoroscopy units were exposed to a median effective radiation dose of 17.8 mSv or 12.3 mSv, respectively. No radiation-related adverse events at 90 days were reported.

© RSNA, 2024

Prostatic artery embolization (PAE) is a minimally invasive angiographic procedure that safely and effectively treats lower urinary tract symptoms, urinary retention, and gross hematuria caused by benign prostatic hyperplasia (1). PAE delivers clinical improvements and prostate gland volume reduction similar to those seen with surgical benign prostatic hyperplasia procedures, with low complication rates (2,3). Numerous studies have established long-term sustainability of such improvements (4–6), and multiple North American and European urology and interventional radiology societies have recently confirmed the role of PAE by formally placing it in their benign prostatic hyperplasia treatment algorithms (7–11).

However, the benign prostatic hyperplasia treatment guidelines published by the American Urological Association continue to cite concerns about perceived risks of patient radiation exposure with PAE (11). Such concerns also commonly persist among referring providers considering embolization procedures for their patients (12,13). As with any embolization procedure, fluoroscopic guidance is vital to the safe practice of PAE. Fluoroscopy is important for real-time angiographic mapping of vascular anatomy and tracking of embolic material deposition.

This copy is for personal use only. To order copies, contact *reprints@rsna.org*

Abbreviations

BMI = body mass index, CAK = cumulative air kerma, PAE = prostate artery embolization

Summary

Patients who underwent prostate artery embolization were administered a median effective patient radiation dose of 17.8 mSv and reported no radiation-related adverse events at 90 days.

Key Results

- In this retrospective study of 1476 patients who underwent prostate artery embolization with a fixed interventional (n = 1345) or mobile (n = 131) fluoroscopy unit, the median effective radiation doses were 17.8 mSv (IQR, 10.2–27.9 mSv) and 12.3 mSv (IQR, 8.5–22.0 mSv), respectively.
- Cumulative air kerma and effective radiation dose both correlated positively with patient body mass index (R^2 = 0.15 and 0.17, respectively; both P < .001) and fluoroscopy time (R^2 = 0.16 and 0.08, respectively; both P < .001).

Moreover, the risks of deterministic effects associated with fluoroscopic procedures, such as erythema or epilation, are exceedingly low and are primarily of concern for patients with high body mass index (BMI), for exceptionally challenging procedures, or for proceduralists unfamiliar with practices to reduce radiation dose (14,15). Few case reports have been published regarding radiation-related adverse events following PAE (15). Furthermore, the risks of stochastic effects for embolization procedures administered to an older male patient population who typically undergo PAE are also estimated to be low (16,17).

Nonetheless, the few reports that quantify the actual radiation exposure incurred during PAE, or the associated risks of deterministic or stochastic effects, are limited by sample size and single-center design (15,18,19). One published systematic review evaluated 22 studies reporting PAE radiation exposure data to model the probability of stochastic injury to patients in defined age groups (17). However, substantial heterogeneity in the reported radiation data across those studies limited interpretation of the reported calculations. The current study aimed to quantify the radiation dose and radiation-related adverse events in patients with benign prostatic hyperplasia who underwent PAE performed by experienced practitioners at 10 high-volume PAE centers.

Materials and Methods

Study Sample and Data Collection

This retrospective study included data from experienced PAE operators (≥10 years of PAE experience, with >75 PAE procedures) at 10 high-volume PAE centers from Europe, South America, and the United States. Data were reviewed in Health Insurance Portability and Accountability Act–compliant fashion according to each institution's review board–approved research protocol. Informed consent was waived because this study was retrospective. Formal data use agreements executed between the primary authors' institution and each contributing institution permitted reporting of pooled multi-institutional data.

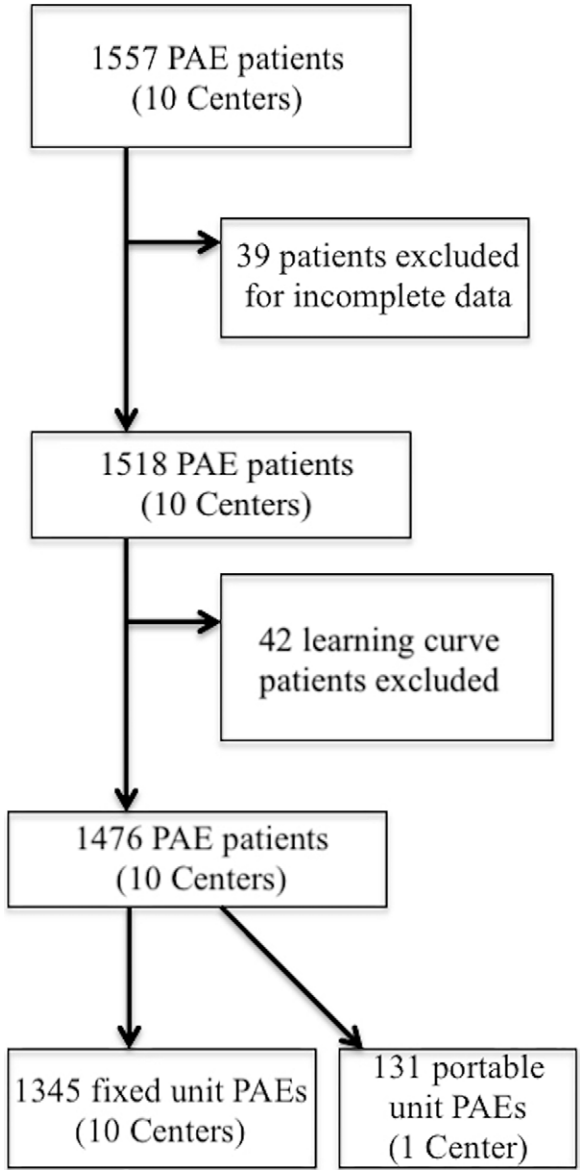

Figure 1: Inclusion and exclusion flow chart. Center 4 submitted data from 131 patients who underwent prostate artery embolization (PAE) procedures performed with a mobile fluoroscopy unit in addition to procedures performed using a fixed interventional unit, and these patients were studied separately.

Contributing centers excluded their first 75 PAE procedures to avoid data skewing by learning curve effects (20). Included were patients age 18 years or older who underwent PAE between January 2014 and May 2021 by each center's lead PAE operator using their fixed interventional fluoroscopic systems and also patients treated at center 4 using mobile fluoroscopy systems. PAE treating benign prostatic hyperplasia–related lower urinary tract symptoms, urinary retention, or gross hematuria were included. Eight centers submitted data from consecutive patients.

Patient age, height, body mass, BMI, year of PAE, presence of radiopaque hip implants, and presence of urinary catheters (placed for chronic retention or per procedural protocol) were documented. Angiographic equipment model and software,

Table 1: Baseline Characteristics of Patients Who Underwent Prostate Artery Embolization, Stratified by Center

Center	Location	No. of Patients	Age (y)	Mass (kg)	Height (m)	BMI	No. of Radiopaque Hip Implants	No. of Urinary Catheters
1	Europe	30	65.0 ± 7.1	78.2 ± 11.5	1.71 ± 0.1	26.8 ± 4.3	0 (0)	0 (0)
2	South America	32	63.3 ± 6.9	82.2 ± 13.8	1.74 ± 0.1	27.0 ± 3.5	0 (0)	2 (6)
3	United States	254	67.5 ± 8.7	85.4 ± 14.9	1.79 ± 0.1	26.5 ± 4.0	15 (6)	10 (4)
4								
Fixed interventional	United States	75	69.5 ± 8.6	86.3 ± 14.4	1.77 ± 0.1	27.0 ± 4.0	8 (11)	7 (9)
Mobile	United States	131	69.9 ± 7.5	85.3 ± 17.0	1.79 ± 0.1	27.3 ± 5.1	8 (6)	7 (5)
5	United States	129	73.5 ± 7.7	87.7 ± 15.5	1.78 ± 0.1	27.7 ± 4.4	8 (6)	39 (30)
6	United States	40	70.5 ± 7.5	83.0 ± 12.0	1.76 ± 0.1	26.7 ± 3.3	3 (8)	5 (13)
7	United States	103	73.5 ± 9.0	83.1 ± 16.2	1.80 ± 0.1	26.9 ± 4.2	3 (3)	30 (29)
8	United States	49	72.1 ± 8.9	83.6 ± 16.6	1.76 ± 0.1	27.0 ± 5.2	4 (8)	9 (18)
9	Europe	106	68.5 ± 10.0	82.9 ± 15.5	1.75 ± 0.1	26.3 ± 4.3	0 (0)	20 (19)
10	United States	527	70.3 ± 9.2	86.2 ± 15.2	1.77 ± 0.1	27.6 ± 4.3	43 (8)	69 (13)

Note.—Continuous data are reported as means ± SDs and categorical data are reported as numbers of patients. Data in parentheses are percentages. Center 4 submitted data separately for fixed interventional and mobile fluoroscopy units. BMI = body mass index (calculated as weight in kilograms divided by height in meters squared).

Table 2: Procedural Data for Prostate Artery Embolization, Stratified by Center

Center	No. of Patients	Unit Manufacturer	Unit Model	Pulse Fluoroscopy (frames per second)	Procedure Time (min)	Radial Access	Technical Success	No. of Access Points	>1 Case	CBCT
1	30	Philips	Allura FD20	7.5	72.8 ± 21.2	20 (67)	30 (100)	1.00 ± 0.0	0 (0)	30 (100)
2	32	GE HealthCare	Innova 4100	7.5	152.6 ± 32.8	0 (0)	32 (100)	1.00 ± 0.0	0 (0)	32 (100)
3	254	Siemens Healthineers	Axiom-Artis	7.5	118.4 ± 38.3	86 (34)	239 (94)	1.01 ± 0.1	0 (0)	175 (69)
4										
Fixed interventional	75	GE HealthCare	630/740	7.5	135.9 ± 54.6	3 (4)	71 (95)	1.00 ± 0.0	3 (4)	74 (99)
Mobile	131	GE HealthCare	OEC Elite	Continuous low dose	95.3 ± 34.1	0 (0)	130 (99)	1.01 ± 0.1	1 (1)	0 (0)
5	129	Philips	Allura Clarity	7.5	151.3 ± 35.4	1 (1)	123 (95)	1.00 ± 0.0	1 (1)	127 (98)
6	40	Siemens Healthineers	Artis Q	7.5	90.8 ± 30.3	38 (95)	36 (90)	1.00 ± 0.0	2 (5)	1 (3)
7	103	GE HealthCare	Discovery IGS 741	7.5	164.0 ± 24.3	1 (1)	84 (82)	1.00 ± 0.0	15 (15)	103 (100)
8	49	Philips	Azurion	7.5	132.9 ± 33.7	6 (13)	48 (98)	1.02 ± 0.1	0 (0)	42 (86)
9	106	Philips/Siemens Healthineers	Azurion/ Axiom-Artis	7.5	90.8 ± 30.2	3 (3)	104 (98)	1.00 ± 0.0	24 (23)	66 (62)
10	527	Siemens Healthineers	Artis Q	7.5	78.9 ± 37.2	474 (90)	506 (96)	1.00 ± 0.0	0 (0)	453 (86)

Note.—Continuous data are reported as means ± SDs and categorical data are reported as numbers of patients; data in parentheses are percentages. Center 4 submitted data separately for fixed interventional and mobile fluoroscopy units. Technical success is defined as complete gland embolization, via unilateral or bilateral prostatic arterial cannulation. Patients who required more than one prostate artery embolization procedure to obtain technical success are noted as ">1 case." CBCT = cone-beam CT.

procedure time (from initial arterial access to closure), fluoroscopy time (cumulative duration of fluoroscopic imaging), fluoroscopy pulse rate, cumulative air kerma (CAK), fluoroscopic field area, and kerma-area product were recorded. Use of cone-beam CT, femoral or radial access, number of access points, and technical success rates (defined as complete gland embolization via unilateral or bilateral prostatic arterial cannulation and from centers submitting consecutive procedure data) were collected. The 90-day radiation-related adverse events were tabulated. Any procedures lacking these data were excluded (Fig 1).

Embolization Procedure

PAE technique consisted of femoral or radial arterial access. Each internal iliac artery was selected with a 5-F angiographic catheter.

Table 3: Radiation Dosimetry during Prostate Artery Embolization Procedures, Stratified by Center

Center	Patients (*n*)	Fluoroscopy Time (min)	CAK (mGy)	Field Area (cm^2)	Kerma-Area Product (Gy · cm^2)	Effective Dose (mSv)
1	30	24.6 ± 9.8	1337 ± 743	158.9 ± 33.5	196.4 (146.4–248.2)	21.6 (16.1–27.3)
2	32	66.0 ± 18.2	1279 ± 656	131.1 ± 21.2	141.8 (109.1–207.3)	15.6 (12.0–22.8)
3	254	39.3 ± 15.4	1725 ± 1219	144.0 ± 160.9	178.2 (113.6–256.4)	19.6 (12.5–28.2)
4						
Fixed interventional	75	34.5 ± 11.1	1652 ± 1095	134.7 ± 23.7	185.5 (125.5–278.2)	20.4 (13.8–30.6)
Mobile	131	33.8 ± 12.7	511 ± 318	297.1 ± 78.0	111.8 (77.3–200.0)	12.3 (8.5–22.0)
5	129	37.5 ± 10.8	2168 ± 1114	133.8 ± 26.0	246.4 (190.0–328.2)	27.1 (20.9–36.1)
6	40	36.0 ± 17.3	1165 ± 1185	216.6 ± 54.7	154.5 (90.0–273.6)	17.0 (9.9–30.1)
7	103	52.6 ± 17.5	557 ± 352	139.4 ± 35.4	61.8 (47.3–87.3)	6.8 (5.2–9.6)
8	49	46.8 ± 11.0	1281 ± 709	234.5 ± 26.0	247.2 (173.6–387.3)	27.2 (19.1–42.6)
9	106	31.5 ± 12.9	483 ± 552	186.5 ± 57.7	54.5 (37.3–82.7)	6.0 (4.1–9.1)
10	527	32.8 ± 14.4	1501 ± 1153	149.1 ± 45.6	169.1 (110.9–259.1)	18.6 (12.2–28.5)
All centers (excluding mobile)	1345	37.2 ± 16.1	1437 ± 1142	153.1 ± 82.7	161.8 (92.7–253.6)	17.8 (10.2–27.9)

Note.—Data are reported as means ± SDs, except effective dose data, which are reported as medians with IQRs in parentheses. Center 4 submitted procedure data separately for fixed interventional and mobile fluoroscopy units. Data compiled for the mobile procedures from center 4 were not included in the overall means and medians. CAK = cumulative air kerma.

Each prostatic artery was subselected using a coaxial microcatheter. Cone-beam CT was performed as needed to delineate arterial anatomy. When necessary, nontarget vessels were protected by coil-embolization blockade. PAE to stasis was performed with 100–300-μm or 300–500-μm trisacryl gelatin spherical particles (Embosphere; Merit Medical Systems). After angiographic catheter removal, hemostasis was obtained with manual compression, vascular closure device, or radial compression band.

Calculation of Effective Dose

CAK (in milligrays), a surrogate for peak skin dose (in milligrays), was used as a predictor of deterministic radiation effects from PAE, although CAK typically overestimates peak skin dose (14,21). Kerma-area product (in grays per centimeters squared), defined as total dose absorbed by irradiated portions of the body, was used as a predictor of stochastic radiation effects (14,21). Effective dose (in millisieverts) is a calculated estimate of stochastic radiation exposure risk that incorporates standardized weighting factors for radiation type administered and body tissue radiosensitivity. A conversion factor, 0.11 mSv/Gy · cm^2, derived from established normalized effective doses from abdominopelvic fluoroscopy-guided procedures (22,23) was used (K.G., A.M.; 3 and 25 years of experience, respectively) to calculate best estimates of effective doses for PAE procedures, as follows: PAE effective dose = (kerma-area product) × 0.11 mSv/Gy · cm^2.

Calculated effective doses for PAE were compared with the effective dose of a standard contrast-enhanced abdominopelvic CT examination. Excess relative risk of cancer-related death from PAE-associated radiation exposure was calculated using an established extrapolation model (24,25). Center 5 also acquired peak skin doses using dose-tracking software (Radimetrics; Bayer Healthcare) to calculate peak skin dose–to-CAK ratios.

Statistical Analysis

Qualitative evaluation of baseline characteristics of the study population was followed by quantitative analysis of any observed heterogeneity that may have affected study results. Procedure time, fluoroscopy time, CAK, and kerma-area product were plotted against sequential procedure number to screen for learning curves among centers that submitted sequential data, and then inputted into a piecewise linear segmented regression model with optimal break-point selection to determine operator learning curve inflection points (20). Procedures occurring before these points were excluded. Median effective doses with IQRs were determined for each center and the overall study sample because of variable center sample sizes and nonnormal data distribution with high-value outliers (both within and among centers) and to facilitate comparisons with established benchmarks (26). Linear regression analyses assessed relationships between CAK or effective dose and patient BMI (calculated as weight in kilograms divided by height in meters squared), fluoroscopy time, or radiation field size at each center for procedures performed with fixed interventional units. Subgroup analyses assessed for effects on effective dose measurements of radiopaque hip implants or indwelling urinary catheters (eliminating radiopaque contrast agent accumulation in the bladder) using Wilcoxon rank sum tests. Because mobile fluoroscopy units had imaging physics fundamentally different from those of fixed interventional systems, radiation dose data from mobile units of center 4 were excluded from overall study sample calculations. Instead, two-sample *t* tests and Wilcoxon rank sum tests were used to compare intracenter differences in radiation doses between fixed interventional and mobile systems. An author (L.H.S.) and another statistician performed analyses using

software (R version 4.0.0; packages Stats version 4.0.0, MASS version 7.3–51.5; R Foundation for Statistical Computing). $P < .05$ indicated statistically significant differences.

Results

Patient and Procedural Data

A total of 1557 patients with PAE procedural data submitted from 10 participating centers were considered for inclusion in this study. After exclusion of 39 procedures for incomplete data and 42 procedures following operator learning curve screening, 1476 patients (mean age, 69.9 years ± 9.0 [SD]) were ultimately included (Fig 1). Baseline patient data stratified by each contributing center are in Table 1. Center 4 submitted data in two groups: 75 patients who underwent the procedure with a fixed interventional fluoroscopy unit and 131 patients who underwent the procedure with a mobile fluoroscopy unit (Fig 1). Body mass, height, and BMI did not differ among any of the sites. Patients from centers 1, 2, and 3 were younger than those treated at the other centers (Table 1). Among the centers, 92 of 1476 patients (6.2%; range, 0.0%–10.6%) had radiopaque hip implants and 198 of 1476 patients (13.4%; range, 0.0%–30.2%) had indwelling urinary catheters. No center routinely placed urinary catheters for procedures.

PAE procedural data stratified by center are shown in Table 2. Overall mean procedure time was 119.3 minutes ± 33.0 (range, 72.8–168.3 minutes). Mean technical success rate was 95% ± 5 (range, 82%–100%). Five centers used cone-beam CT for 98%–100% of procedures, whereas the other five centers used cone-beam CT for 3%–86% of procedures. Three centers used radial access in most procedures (range, 67%–95%); seven centers used it in a minority of procedures (range, 0%–34%).

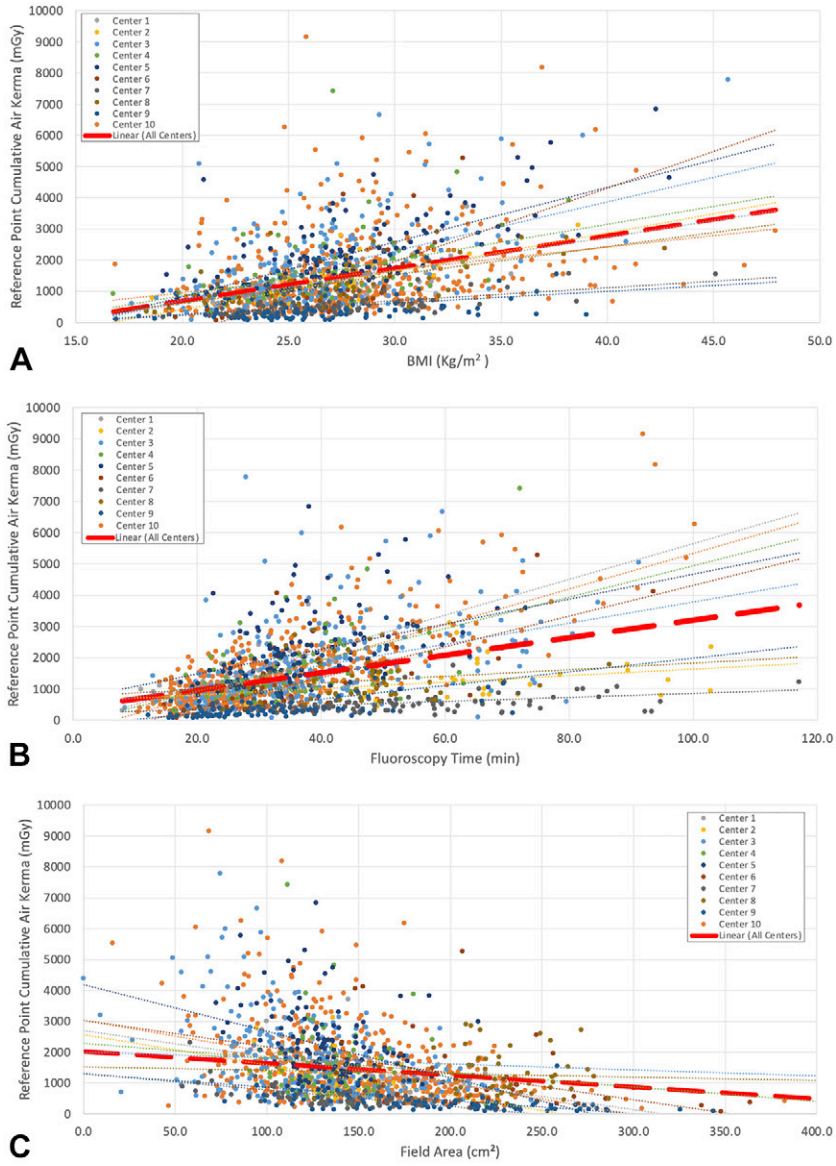

Figure 2: Scatterplots show the relationship between cumulative air kerma (CAK) and **(A)** patient body mass index (BMI), **(B)** fluoroscopy time in minutes, and **(C)** field area in centimeters squared for fixed interventional unit prostate artery embolization procedures from all centers ($n = 1345$). There is a positive correlation between CAK and BMI ($\beta = 104.48$; $R^2 = 0.15$; $P < .001$) and CAK and fluoroscopy time ($\beta = 28.19$; $R^2 = 0.16$; $P < .001$). There is a negative correlation between CAK and procedure field area ($\beta = -3.84$; $R^2 = 0.08$; $P < .001$). Red dashed lines are trend lines for data from all 10 centers; smaller dotted lines are trend lines for individual centers.

Radiation Dose Data

PAE radiation dose data for 1476 PAE procedures stratified by center are in Table 3. The overall median effective dose was 17.8 mSv for procedures performed with fixed interventional fluoroscopy units ($n = 1345$; IQR, 10.2–27.9 mSv) and 12.3 mSv for procedures performed using mobile fluoroscopy units ($n = 131$; IQR , 8.5–22.0 mSv). No centers reported deterministic-type or stochastic-type adverse events from radiation exposure within 90 days after PAE. CAK less than 2 Gy typically causes no observable adverse effects, whereas CAK of 2–5 Gy may cause temporary erythema or epilation (14). Nine of 10 centers reported mean PAE CAK values less than 2 Gy, and 24 of 1476 (1.6%) procedures had CAK greater than 5 Gy. The International Commission on Radiological Protection provides extrapolation models for estimation of relative risk of cancer-related death from procedure-related radiation, estimating such risk to be 4.1%–4.8% per sievert of effective dose in adults (24,25). For the current study, a median 0.07%–0.09% excess relative risk of cancer-related death associated with PAE was calculated.

For fixed interventional unit procedures, CAK demonstrated a positive correlation with BMI ($\beta = 104.48$; $R^2 = 0.15$; $P < .001$) and fluoroscopy time ($\beta = 28.19$; $R^2 = 0.16$; $P < .001$)

and a negative correlation with procedure field area (β = −3.84; R^2 = 0.08; P < .001) (Fig 2). Effective dose values from fixed interventional unit procedures also demonstrated a positive correlation with patient BMI (β = 1.50; R^2 = 0.17; P < .001) and fluoroscopy time (β = 0.27; R^2 = 0.08; P < .001) and a negative correlation with procedure field area (β = −0.003; R^2 = 0.002; P < .03) (Fig 3). Therefore, measures of radiation dose that predict both deterministic and stochastic effects correlated positively with BMI and fluoroscopy time. Effective dose showed strong positive correlation with CAK (β = 0.01; R^2 = 0.72; P < .001) (Fig 4).

At center 5, 20 of 129 procedures (15.5%) resulted in CAK values of 3000 mGy or higher. Calculated peak skin doses for these procedures were lower than the CAK values (2580 mGy ± 641 vs 4010 mGy ± 990, respectively; P < .001). The peak skin dose–to-CAK ratio decreased with increasing radiation dose distribution (Fig 5).

Radiopaque Implants and Fixed Interventional versus Mobile Fluoroscopy Units

Among centers from which study samples contained a subset of patients with radiopaque hip implants, median CAK was higher for patients with implants versus those without implants (1452 mGy [IQR, 900–2685 mGy] vs 1177 mGy [IQR, 700–1959 mGy], respectively; P < .01). Median CAK did not differ when a urinary catheter was present versus absent (1208 mGy [IQR, 548–1953 mGy] vs 1192 mGy [IQR, 735–2000 mGy], respectively; P = .09).

At center 4, patient age and BMI at baseline did not differ between patients who underwent PAE with a fixed interventional unit and those who did so with a mobile fluoroscopy unit (P = .76 and P = .68, respectively) (Table 4). Procedure time was shorter for mobile units than for fixed units (95.3 minutes ± 34.1 vs 135.9 minutes ± 54.6, respectively; P < .001), but no difference in fluoroscopy times was observed between the unit types (P = .67). The mean field of view size was larger for mobile versus fixed unit procedures (297.1 cm² ± 78.0 vs 134.7 cm² ± 23.7, respectively; P < .001). For PAE procedures performed with mobile units, mean CAK (510.8 mGy ± 318.1), median kerma-area product (112.0 Gy · cm²; range, 77.3–200.0 Gy · cm²), and median effective dose (12.3 mSv; range, 8.5–22.0 mSv) were lower than those from the fixed interventional unit (CAK, 1651.6 mGy ± 1094.5; kerma-area product, 185.2 Gy · cm² [range, 125.5–278.4 Gy · cm²]; effective dose, 20.4 mSv [range, 13.8–30.6 mSv]; P < .001 for all) (Table 4).

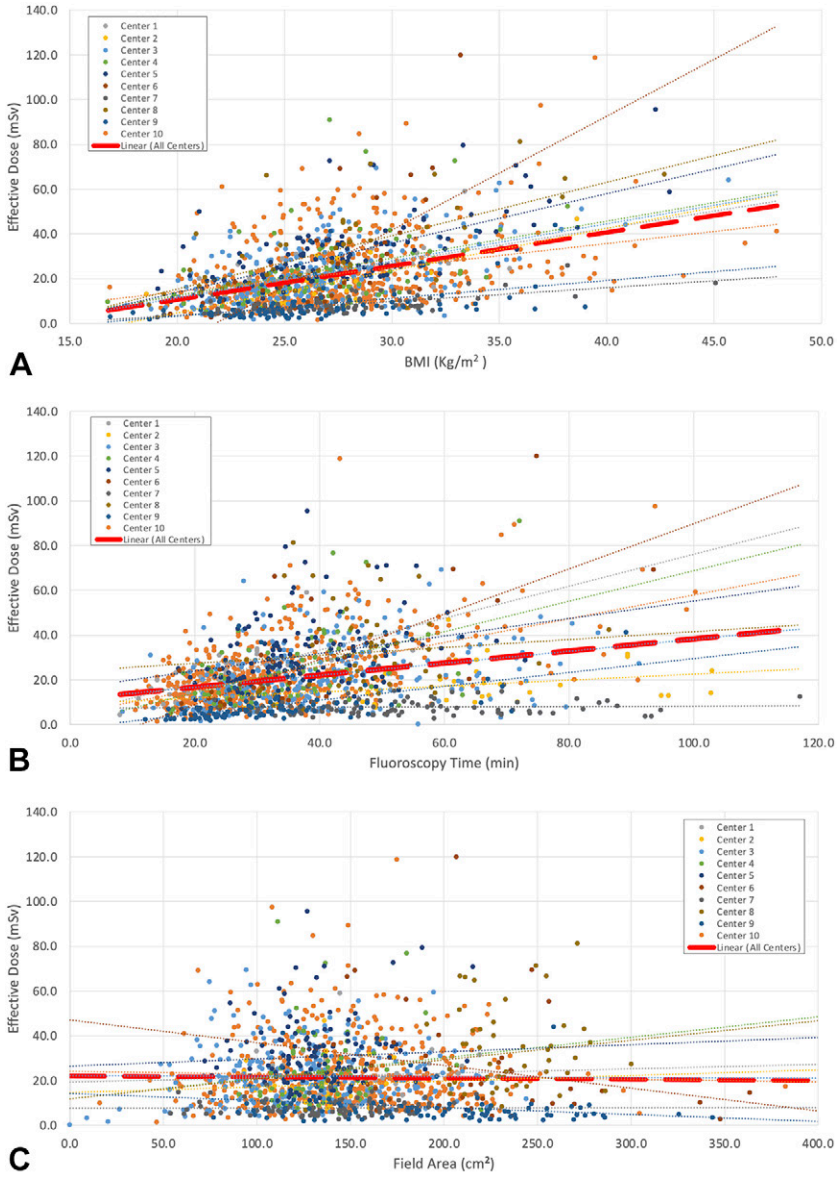

Figure 3: Scatterplots show the relationship between effective dose and **(A)** patient body mass index (BMI), **(B)** fluoroscopy time in minutes, and **(C)** field area in centimeters squared for fixed interventional unit prostate artery embolization procedures from all centers (n = 1345). A positive correlation is seen between effective dose and BMI (β = 1.50; R^2 = 0.17; P < .001) and between effective dose and fluoroscopy time (β = 0.27; R^2 = 0.08; P < .001). A negative correlation is seen between effective dose and procedure field area (β = −0.003; R^2 = 0.002; P < .03). Red dashed lines are trend lines for data from the 10 centers; smaller dotted lines are trend lines for individual centers.

Discussion

To our knowledge, only small, single-center studies have reported radiation doses for patients with benign prostatic hyperplasia undergoing treatment with prostate artery embolization (PAE). Our study aimed to quantify the radiation exposure incurred during PAE using data from procedures performed by experienced providers using a similar technique at 10 high-volume centers that perform PAE. The observed median effective radiation dose of PAE with fixed interventional fluoroscopy units was 17.8 mSv (range, 10.2–27.9 mSv) and 12.3 mSv (range, 8.5–22.0 mSv) with mobile fluoroscopy units. Cumulative air kerma and effective dose both correlated positively with patient

body mass index (R^2 = 0.15 and 0.17; P < .001 for both) and fluoroscopy time (R^2 = 0.16 and 0.08; P < .001 for both).

To place these effective dose data in the context of a radiologic examination that medical practitioners and patients may be familiar with, PAE effective dose was compared with the effective dose of contrast-enhanced abdominopelvic CT, which images the same body area using a similar contrast-enhanced technique with a well-established effective dose profile. The established achievable dose-length product of 608 mGy · cm for such an examination corresponds to the 50th percentile of nationally reported doses (26,27). Converting this value using the established 0.015 mSv/Gy · cm conversion factor yields a derived median effective dose of 9.1 mSv for this type of examination (28). Therefore, our study's median PAE effective dose of 17.8 mSv was less than the effective dose sum of two contrast-enhanced abdominopelvic CT examinations and less than three times the mean annual environmental radiation exposure of 6.2 mSv for a person residing in the United States (including 3.1 mSv from medical sources and 2.6 mSv from normal physiologic breathing and ingestion) (29). Moreover, our study sample demonstrated no 90-day deterministic effects from PAE radiation exposure.

A systematic review (17) of radiation exposure risks from 22 published PAE series showed a mean kerma-area product of 181.6 Gy · cm^2 and a mean effective dose of 28.3 mSv, compared with our reported median kerma-area product of 161.8 Gy · cm^2 and median effective dose of 17.8 mSv. Zumstein et al (17) further calculated that their mean effective dose would contribute 0.12% excess relative risk of cancer-related death in a 66-year-old patient. Considering our study's lower median effective dose, lower median excess relative risk of cancer-related death of 0.07%–0.09%, and older mean patient age, the stochastic risks related to PAE in this study sample would be even lower. Because such cancer-related deaths typically occur more than 15 years

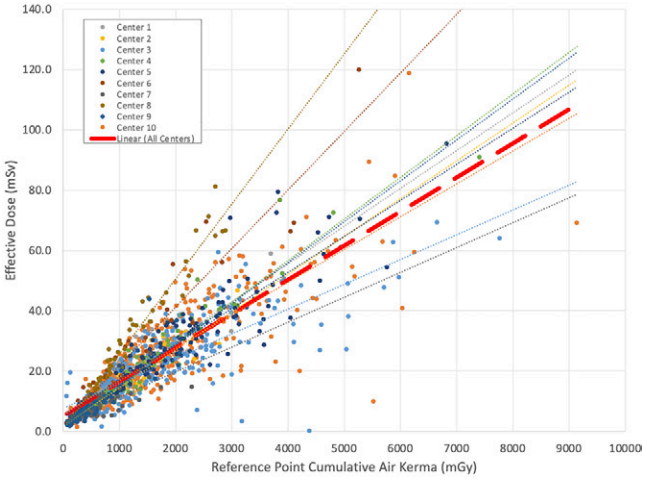

Figure 4: Scatterplot shows a strong positive correlation between effective dose and cumulative air kerma (β = 0.01; R^2 = 0.72; P < .001) for fixed interventional unit prostate artery embolization procedures at the 10 centers (n = 1345). The red dashed line is a trend line for data from all centers; the smaller dotted lines are trend lines for individual centers.

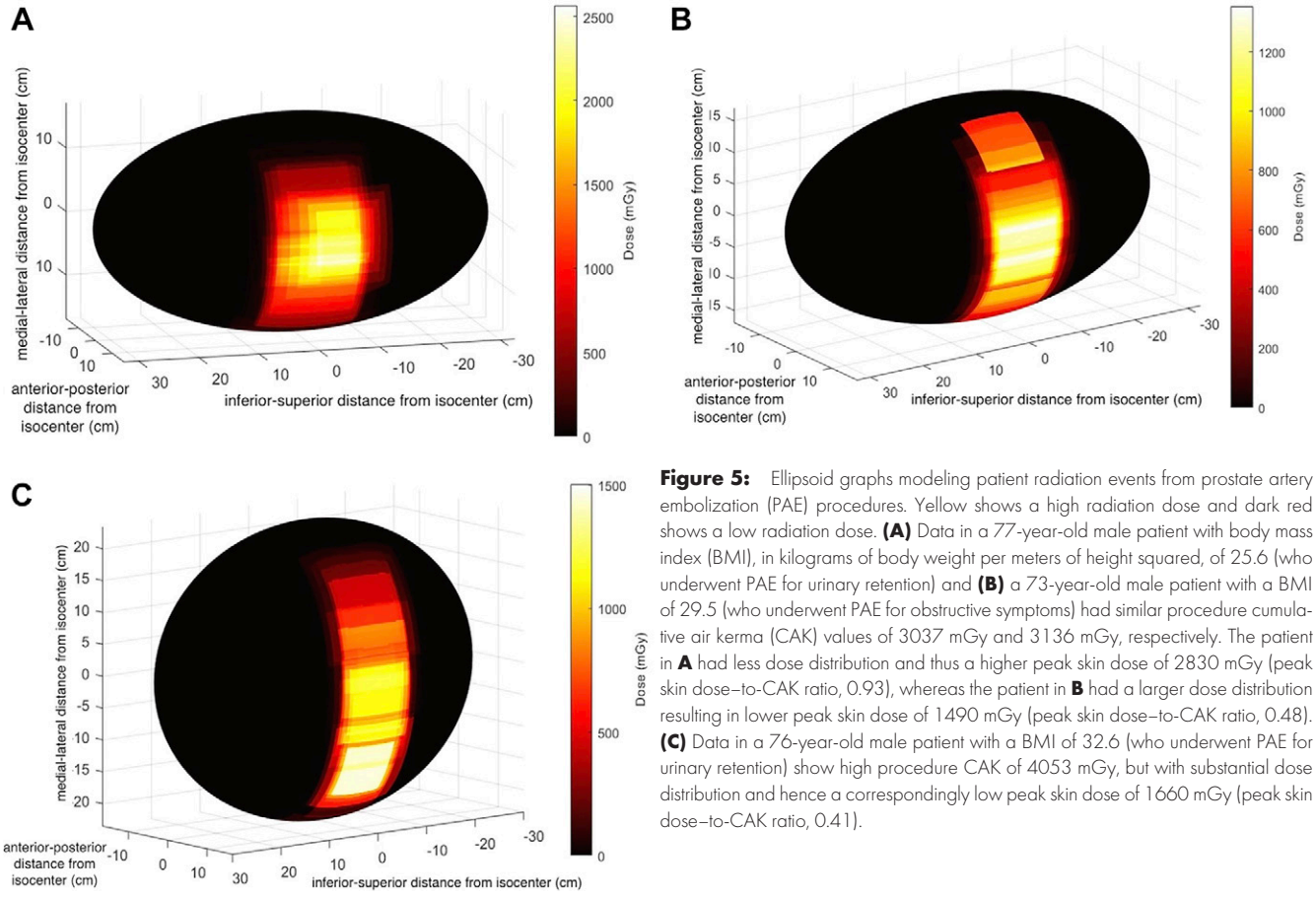

Figure 5: Ellipsoid graphs modeling patient radiation events from prostate artery embolization (PAE) procedures. Yellow shows a high radiation dose and dark red shows a low radiation dose. **(A)** Data in a 77-year-old male patient with body mass index (BMI), in kilograms of body weight per meters of height squared, of 25.6 (who underwent PAE for urinary retention) and **(B)** a 73-year-old male patient with a BMI of 29.5 (who underwent PAE for obstructive symptoms) had similar procedure cumulative air kerma (CAK) values of 3037 mGy and 3136 mGy, respectively. The patient in **A** had less dose distribution and thus a higher peak skin dose of 2830 mGy (peak skin dose–to-CAK ratio, 0.93), whereas the patient in **B** had a larger dose distribution resulting in lower peak skin dose of 1490 mGy (peak skin dose–to-CAK ratio, 0.48). **(C)** Data in a 76-year-old male patient with a BMI of 32.6 (who underwent PAE for urinary retention) show high procedure CAK of 4053 mGy, but with substantial dose distribution and hence a correspondingly low peak skin dose of 1660 mGy (peak skin dose–to-CAK ratio, 0.41).

Table 4: Prostate Artery Embolization Procedure Data from Center 4

Parameter	Fixed Unit (n = 75)	Mobile Unit (n = 131)	P Value
Age (y)	69.5 ± 8.6	69.9 ± 7.5	.76
BMI	27.0 ± 4.0	27.3 ± 5.13	.68
Procedure time (min)	135.9 ± 54.6	95.3 ± 34.1	<.001
Fluoroscopy time (min)	34.5 ± 11.1	33.8 ± 12.7	.67
CAK (mGy)	1651.6 ± 1094.5	510.8 ± 318.1	<.001
Field area (cm^2)	134.7 ± 23.7	297.1 ± 78.0	<.001
Kerma-area product (Gy · cm^2)	185.2 (125.5–278.4)	112.0 (77.3–200.0)	<.001
Effective dose (mSv)	20.4 (13.8–30.6)	12.3 (8.5–22.0)	<.001

Note.—Patient characteristics and procedural parameters for fixed interventional unit versus mobile unit data are reported as means ± SDs and compared using two-sample t tests. Kerma-area product and effective dose are reported as medians with IQRs in parentheses and were compared using Wilcoxon rank sum tests. Procedure time spans initial arterial access to access closure; fluoroscopy time is the cumulative duration of fluoroscopic imaging. BMI = body mass index (calculated as weight in kilograms divided by height in meters squared), CAK = cumulative air kerma.

after exposure and most patients undergo PAE after age 60 years, this excess relative risk realized in the eighth decade of life may have little impact on life expectancy in this population (30).

Despite these reassuring findings, the importance of minimizing radiation exposure during fluoroscopy-guided procedures is paramount. Patient-related factors, including high BMI and radiopaque implants, can increase beam attenuation and photon scatter. In this study, BMI correlated positively with effective dose (β = 1.50; R^2 = 0.17; P < .001) and radiopaque hip implants resulted in higher median CAK (1452 mGy vs 1177 mGy; P < .01). Therefore, counseling regarding such risk factors is important, particularly for patients with obesity. As outlined in the radiation dose management guidelines from the Society of Interventional Radiology, operator-dependent exposure reduction techniques are also critical (14). Although not necessarily a reliable dose index, fluoroscopy time can decrease with increasing operator experience (20). Other factors to optimize include beam collimation, beam magnification, pulse and frame rates, subtraction angiography and cone-beam CT use, and dose distribution. Regarding the fluoroscopic equipment used, the age of the device, dose reduction features, and hardware technology can also impact procedural radiation dose (31). This study demonstrated lower effective dose when PAE was performed using mobile fluoroscopy units compared with PAE performed by the same operator using a fixed interventional unit, although rates of clinical success and non–radiation-related adverse events for the two groups were not compared.

Our study had limitations. First, the retrospective data collection may have impacted quantification of radiation exposure. Second, effective dose calculations were limited by assumptions, estimations, and simplifications inherent to radiation dose quantification. Third, imaging frame rates, cone-beam CT technique variations, and proportional subtraction angiography, cone-beam CT, and fluoroscopy radiation doses were not evaluated. Fourth, data were collected from experienced providers, thus limiting generalizability of our findings to centers with less experienced providers.

Overall, our study showed that patients with benign prostatic hyperplasia who underwent prostate artery embolization (PAE) performed with fixed interventional or mobile fluoroscopy units incurred a median effective radiation dose of 17.8 mSv or 12.3 mSv, respectively, with no radiation-related adverse events reported at 90 days. These findings provide important context for comparing the risks of PAE-related radiation exposure (among other risks of a minimally invasive angiographic procedure) to the trade-off risks of alternative surgical procedures, including erectile dysfunction, incontinence, and other, more severe surgical complications. These findings will allow patients, referring providers, and societal guideline committees to evaluate the merits of PAE more accurately as a procedural option for treatment of benign prostatic hyperplasia. Larger prospective studies stratifying data sets by imaging equipment type, patient body mass index, and individual operator may further inform this evaluation.

Acknowledgments: The authors acknowledge the invaluable assistance with statistical analysis provided by Michele Hacker, ScD (Beth Israel Deaconess Medical Center), and James Sayre, PhD (University of California, Los Angeles). The authors also acknowledge the extensive data collection efforts by Carole Déan, PhD, and Claire Van Ngoc Ty, PhD (both from Hôpital Européen Georges Pompidou), as well as Arthur Diego Doas Rocha, MSc, Andre Moreira de Assis, MD, PhD, and Airton Mota Moreira MD, PhD (all from Universidade de Sao Paulo Faculdade de Medicina).

Author contributions: Guarantors of integrity of entire study, **R.A., S.Z.R., R.S.M., F.C.C., T.M., A.R., H.Y.**; study concepts/study design or data acquisition or data analysis/interpretation, all authors; manuscript drafting or manuscript revision for important intellectual content, all authors; approval of final version of submitted manuscript, all authors; agrees to ensure any questions related to the work are appropriately resolved, all authors; literature research, **R.A., S.Z.R., K.G., A.M., R.S.M., S.B., C.D., T.M., R.S., H.Y.**; clinical studies, **R.A., S.Z.R., K.G., A.M., R.S.M., T.B., F.C.C., C.D., A.R., M.S., H.Y.**; experimental studies, **R.S.M., C.D., C.N.**; statistical analysis, **R.A., S.Z.R., K.G., L.H.S., R.S.M., C.D., R.S.**; and manuscript editing, all authors

Disclosures of conflicts of interest: **R.A.** No relevant relationships. **S.Z.R.** No relevant relationships. **K.G.** No relevant relationships. **A.M.** No relevant relationships. **L.H.S.** No relevant relationships. **R.S.M.** No relevant relationships. **S.B.** Research grant from Merit Medical; stock/stock options from Embolx Medical. **T.B.** Payment or honoraria for lectures from Terumo, Merit, Cook Medical, and Philips. **F.C.C.** No relevant relationships. **C.D.** No relevant relationships. **A.F.** No relevant relationships. **A.I.** Consulting fees from CrannMed; payment or honoraria for lecturres from Terumo; leadership or fiduciary role in other board, society, committee or advocacy group, paid or unpaid, from Boston Scientific. **T.M.** Research support from Angiodynamics; consulting fees from Boston Scientific, Francis Medical, and Johnson and Johnson; leadership role on the Genitourinary Council of the Society of Interventional Radiology. **J.M.** Payment for lectures from Terumo, Penumbra, and Siemens Medical Solutions. **C.N.** Consulting fees from Merit Medical, Varian Medical, GE HealthCare, Sirtex Medical. **A.R.** No relevant relationships. **R.S.** No relevant relationships. **M.S.** No relevant relationships. **H.Y.** No relevant relationships.

References

1. Ray AF, Powell J, Speakman MJ, et al. Efficacy and safety of prostate artery embolization for benign prostatic hyperplasia: an observational study and propensity-matched comparison with transurethral resection of the prostate (the UK-ROPE study). BJU Int 2018;122(2):270–282.

2. Porto JG, Arbelaez MCS, Blachman-Braun R, et al. Complications associated with minimally invasive surgical therapies (MIST) for surgical management of benign prostatic hyperplasia: a Manufacturer and User Facility Device Experience (MAUDE) database review. World J Urol 2023;41(7):1975–1982.
3. Abt D, Hechelhammer L, Müllhaupt G, et al. Comparison of prostatic artery embolisation (PAE) versus transurethral resection of the prostate (TURP) for benign prostatic hyperplasia: randomised, open label, non-inferiority trial. BMJ 2018;361:k2338.
4. Bilhim T, Costa NV, Torres D, Pinheiro LC, Spaepen E. Long-term outcome of prostatic artery embolization for patients with benign prostatic hyperplasia: single-centre retrospective study in 1072 patients over a 10-year period. Cardiovasc Intervent Radiol 2022;45(9):1324–1336.
5. Somwaru AS, Metting S, Flisnik LM, Nellamattathil MG, Sharma A, Katabathina VS. Prostate artery embolization has long term efficacy for treatment of severe lower urinary tract symptoms from giant prostatic hyperplasia. BMC Urol 2020;20(1):153.
6. Ayyagari R, Powell T, Staib L, et al. Prostatic artery embolization using 100-300-μm trisacryl gelatin microspheres to treat lower urinary tract symptoms attributable to benign prostatic hyperplasia: a single-center outcomes analysis with medium-term follow-up. J Vasc Interv Radiol 2020;31(1):99–107.
7. McWilliams JP, Bilhim TA, Carnevale FC, et al. Society of Interventional Radiology multisociety consensus position statement on prostatic artery embolization for treatment of lower urinary tract symptoms attributed to benign prostatic hyperplasia: from the Society of Interventional Radiology, the Cardiovascular and Interventional Radiological Society of Europe, Société Française de Radiologie, and the British Society of Interventional Radiology: Endorsed by the Asia Pacific Society of Cardiovascular and Interventional Radiology, Canadian Association for Interventional Radiology, Chinese College of Interventionalists, Interventional Radiology Society of Australasia, Japanese Society of Interventional Radiology, and Korean Society of Interventional Radiology. J Vasc Interv Radiol 2019;30(5):627–637.e1.
8. Cornelis FH, Bilhim T, Hacking N, Sapoval M, Tapping CR, Carnevale FC. CIRSE standards of practice on prostatic artery embolisation. Cardiovasc Intervent Radiol 2020;43(2):176–185.
9. Gravas S, Gacci M, Gratzke C, et al. Summary paper on the 2023 European Association of Urology Guidelines on the management of non-neurogenic male lower urinary tract symptoms. Eur Urol 2023;84(2):207–222.
10. NICE Guidance - Prostate artery embolisation for lower urinary tract symptoms caused by benign prostatic hyperplasia: © NICE (2018) Prostate artery embolisation for lower urinary tract symptoms caused by benign prostatic hyperplasia. BJU Int 2018;122(1):11–12.
11. Sandhu JS, Bixler BR, Dahm P, et al. Management of lower urinary tract symptoms attributed to benign prostatic hyperplasia (BPH): AUA guideline amendment 2023. J Urol 2024;211(1):11–19.
12. Sacks B, Meyerson G, Siegel JA. Epidemiology without biology: false paradigms, unfounded assumptions, and specious statistics in radiation science (with commentaries by Inge Schmitz-Feuerhake and Christopher Busby and a reply by the authors). Biol Theory 2016;11(2):69–101.
13. Oakley PA, Harrison DE. X-ray hesitancy: patients' radiophobic concerns over medical x-rays. Dose Response 2020;18(3):1559325820959542.
14. Stecker MS, Balter S, Towbin RB, et al. Guidelines for patient radiation dose management. J Vasc Interv Radiol 2009;20(7 Suppl):S263–S273.
15. Laborda A, De Assis AM, Ioakeim I, Sánchez-Ballestín M, Carnevale FC, De Gregorio MA. Radiodermitis after prostatic artery embolization: case report and review of the literature. Cardiovasc Intervent Radiol 2015;38(3):755–759.
16. O'Brien B, van der Putten W. Quantification of risk-benefit in interventional radiology. Radiat Prot Dosimetry 2008;129(1-3):59–62.
17. Zumstein V, Binder J, Güsewell S, et al. Radiation exposure during prostatic artery embolisation: a systematic review and calculation of associated risks. Eur Urol Focus 2021;7(3):608–611.
18. Andrade G, Khoury HJ, Garzón WJ, et al. Radiation exposure of patients and interventional radiologists during prostatic artery embolization: a prospective single-operator study. J Vasc Interv Radiol 2017;28(4):517–521.
19. Kriechenbauer BMT, Franiel T, Bürckenmeyer F, et al. Influence of interventionists' experience on radiation exposure of patients who underwent prostate artery embolization: 4-year results from a retrospective, single-center study. Cardiovasc Intervent Radiol 2020;43(8):1194–1201.
20. Powell T, Rahman S, Staib L, Bhatia S, Ayyagari R. Operator learning curve for prostatic artery embolization and its impact on outcomes in 296 patients. Cardiovasc Intervent Radiol 2023;46(2):229–237.
21. Valentin J. Avoidance of radiation injuries from medical interventional procedures. Ann ICRP 2000;30(2):7–67.
22. Smans K, Struelens L, Hoornaert MT, et al. A study of the correlation between dose area product and effective dose in vascular radiology. Radiat Prot Dosimetry 2008;130(3):300–308.
23. NCRP Report No. 168, Radiation dose management for fluoroscopically-guided interventional medical procedures. https://ncrponline.org/publications/reports/ncrp-report-168/. Published 2015. Accessed November 7, 2023.
24. The 2007 Recommendations of the International Commission on Radiological Protection. ICRP publication 103. Ann ICRP 2007;37(2-4):1–332.
25. 1990 Recommendations of the International Commission on Radiological Protection. Ann ICRP 1991;21(1-3):1–201.
26. American College of Radiology, American Association of Physicists in Medicine, Society for Pediatric Radiology. Practice parameter for diagnostic reference levels and achievable doses in medical x-ray imaging. American College of Radiology Website. https://www.acr.org/-/media/ACR/Files/Practice-Parameters/diag-ref-levels.pdf. Published 2018. Accessed February 17, 2023.
27. Kanal KM, Butler PF, Sengupta D, Bhargavan-Chatfield M, Coombs LP, Morin RL. U.S. diagnostic reference levels and achievable doses for 10 adult CT examinations. Radiology 2017;284(1):120–133.
28. McCollough C, Cody D, Edyvean S, et al. Report No. 096 - The Measurement, Reporting, and Management of Radiation Dose in CT. https://www.aapm.org/pubs/reports/RPT_96.pdf. Published 2008. Accessed March 24, 2023.
29. Wall BF. Ionising radiation exposure of the population of the United States: NCRP Report No. 160. Radiat Prot Dosimetry 2009;136(2):136–138.
30. Preston DL, Shimizu Y, Pierce DA, Suyama A, Mabuchi K. Studies of mortality of atomic bomb survivors. Report 13: Solid cancer and noncancer disease mortality: 1950-1997. Radiat Res 2003;160(4):381–407.
31. Hill KD, Mann SD, Carboni MP, et al. Variability in radiation dose and image quality: a comparison across fluoroscopy-system vendors, generations of equipment and institutions. Catheter Cardiovasc Interv 2018;92(7):E471–E477.